

Dear Prof. Nizkorodov,

Thank you very much for your time, and particularly for your careful reading and valuable suggestion. We have made all changes accordingly. Thank you again!

Lines 33: those show -> compounds that have

Response: Change made.

Lines 35: those show -> compounds that have a

Response: Change made.

Sentence on line 42 in spring, in fall, in winter, in summer should be at the end of each statement

Response: Change made.

Line 71: some of the papers by Lin reported contribution of resolved compounds to the overall absorption coefficient that was considerably higher than reported here. It might be worth citing these numbers. For example, Lin (2017) attributes about 50% of the total absorption to nitroaromatics. Do you have any suggestions why his numbers could be so different from numbers reported here?

Response: This is indeed a very good question. Lin et al. (2016) reported that in biofuels burning samples (sawgrass, peat, ponderosa pine, and black spruce), 40-60% of the bulk BrC absorption in the wavelength range of 300-500 nm may be attributed to 20 strong chromophores. Also, Lin et al. (2017) reported that during the biomass burning event (Lag Ba'Omer, a nationwide bonfire festival in Israel), nitroaromatic compounds accounted for ~50% of the total absorption of water-soluble BrC. These numbers are considerably higher than that reported in our study. The differences could be due to that the samples measured in Lin et al. (2016; 2017) were from biofuels burning or biomass

burning event with abundant emissions of aromatic compounds which can be transformed to nitroaromatics through chemical reactions (Harrison et al., 2005; Mazzoleni et al., 2007; Stockwell et al., 2014), whereas our samples were from urban air with mixed sources. In addition, Lin et al. measured the contribution not from the specific compounds but over 20 elemental formulas which could have dozens or even hundred of structures and we measured the contribution from 25 specific compounds. Furthermore, in Lin et al. (2017), they calculated the contribution to light absorption of water-soluble BrC and We calculated the contribution to methanol-soluble BrC which is ~2 times higher than light absorption of water-soluble BrC.

We have now cited these numbers from Lin et al. (2016, 2017). In line 72-77, it now reads "... Lin et al. (2016) reported that in biofuels burning samples (sawgrass, peat, ponderosa pine, and black spruce), about 40-60% of the bulk BrC absorption in the wavelength range of 300-500 nm may be attributed to 20 strong chromophores and in another study (Lin et al., 2017) they reported that nitroaromatic compounds accounted for ~50% of the total absorption of water-soluble BrC during the biomass burning event in a nationwide bonfire festival in Israel."

Line 164-165: are -> were

Response: Change made.

Line 178: LOD (limit of detection) is a more common term

Response: Change made.

Line 216: compounds with high conjugation degree and strong light-absorbing capability (e.g., PAHs) at longer wavelength-> conjugated compounds that absorb strongly at longer wavelengths (e.g., PAHs)

Response: Change made.

Figure 1 appears very grainy on my computer, I would recommend uploading a higher resolution version in the final revision

Response: Thank you for your suggestion. We have provided a new version with higher resolution.

Figure 2: the red box showing results of this study and black dotted lines separating different types of sites may be hard to see; it may be worth making them thicker

Response: Thank you for your suggestion. We have made the red box and black dotted lines thicker in Figure 2.

References

- Harrison, M. A. J., Barra, S., Borghesi, D., Vione, D., Arsene, C., and Olariu, R. I.: Nitrated phenols in the atmosphere: a review, *Atmos. Environ.*, 39, 231–248, 2005.
- Mazzoleni, L. R., Zielinska, B., and Moosmuller, H.: Emissions of levoglucosan, methoxy phenols, and organic acids from prescribed burns, laboratory combustion of wildland fuels, and residential wood combustion, *Environ. Sci. Technol.*, 41, 2115–2122, 2007.
- Stockwell, C. E., Yokelson, R. J., Kreidenweis, S. M., Robinson, A. L., DeMott, P. J., Sullivan, R. C., Reardon, J., Ryan, K. C., Griffith, D. W. T., and Stevens, L.: Trace gas emissions from combustion of peat, crop residue, domestic biofuels, grasses, and other fuels: configuration and Fourier transform infrared (FTIR) component of the fourth Fire Lab at Missoula Experiment (FLAME-4), *Atmos. Chem. Phys.*, 14, 9727–9754, 2014.

1 **Characterization of the light absorbing properties, chromophores composition**
2 **and sources of brown carbon aerosol in Xi'an, Northwest China**

3 Wei Yuan^{1,2}, Ru-Jin Huang^{1,3}, Lu Yang¹, Jie Guo¹, Ziyi Chen⁴, Jing Duan^{1,2}, Meng Wang^{1,2}, Ting
4 Wang^{1,2}, Haiyan Ni¹, Yongming Han¹, Yongjie Li⁵, Qi Chen⁶, Yang Chen⁷, Thorsten Hoffmann⁸,
5 Colin O'Dowd⁹

6 ¹State Key Laboratory of Loess and Quaternary Geology, Center for Excellence in Quaternary
7 Science and Global Change, Chinese Academy of Sciences, and Key Laboratory of Aerosol
8 Chemistry & Physics, Institute of Earth Environment, Chinese Academy of Sciences, Xi'an
9 710061, China

10 ²University of Chinese Academy of Sciences, Beijing 100049, China

11 ³Institute of Global Environmental Change, Xi'an Jiaotong University, Xi'an 710049, China

12 ⁴Royal School of Mines, South Kensington Campus, Imperial College London, Exhibition
13 Road, London SW7 3RW, United Kingdom

14 ⁵Department of Civil and Environmental Engineering, Faculty of Science and Technology,
15 University of Macau, Taipa, Macau 999078, China

16 ⁶State Key Joint Laboratory of Environmental Simulation and Pollution Control, College of
17 Environmental Sciences and Engineering, Peking University, Beijing 100871, China

18 ⁷Chongqing Institute of Green and Intelligent Technology, Chinese Academy of Sciences,
19 Chongqing 400714, China

20 ⁸Institute of Inorganic and Analytical Chemistry, Johannes Gutenberg University Mainz,
21 Duesbergweg 10–14, Mainz 55128, Germany

22 ⁹School of Physics and Centre for Climate and Air Pollution Studies, Ryan Institute, National
23 University of Ireland Galway, University Road, Galway H91CF50, Ireland

24 *Correspondence to:* Ru-Jin Huang (rujin.huang@ieecas.cn)

25 **Abstract**

26 The impact of brown carbon aerosol (BrC) on the Earth's radiative forcing balance has

27 been widely recognized but remains uncertain, mainly because the relationships among BrC
28 sources, chromophores, and optical properties of aerosol are poorly understood. In this work,
29 the light absorption properties and chromophore composition of BrC were investigated for
30 samples collected in Xi'an, Northwest China from 2015 to 2016. Both absorption Ångström
31 exponent and mass absorption efficiency show distinct seasonal differences, which could be
32 attributed to the differences in sources and chromophore composition of BrC. Three groups of
33 light-absorbing organics were found to be important BrC chromophores, including [compounds](#)
34 [that have these show](#) multiple absorption peaks at wavelength > 350 nm (12 polycyclic aromatic
35 hydrocarbons and their derivatives) and [compounds that have these show](#) single absorption
36 peak at wavelength < 350 nm (10 nitrophenols and nitrosalicylic acids and 3 methoxyphenols).
37 These measured BrC chromophores show distinct seasonal differences and contribute on
38 average about 1.1% and 3.3% of light absorption of methanol-soluble BrC at 365 nm in summer
39 and winter, respectively, about 7 and 5 times higher than the corresponding carbon mass
40 fractions in total organic carbon. The sources of BrC were resolved by positive matrix
41 factorization (PMF) using these chromophores instead of commonly used non-light absorbing
42 organic markers as model inputs. Our results show that ~~in spring~~ vehicular emissions and
43 secondary formation are major sources of BrC (~70%) [in spring](#), ~~in fall~~ coal combustion and
44 vehicular emissions are major sources (~70%) [in fall](#), ~~in winter~~ biomass burning and coal
45 combustion become major sources (~80%) [in winter](#), while ~~in summer~~ secondary BrC
46 dominates (~60%) [in summer](#).

47 **1 Introduction**

48 Brown carbon (BrC) is an important component of atmospheric aerosol particles and has
49 significant effects on radiative forcing and climate (Feng et al., 2013; Laskin et al., 2015; Zhang
50 et al., 2017a). BrC can efficiently absorb solar radiation and reduce the photolysis rates of
51 atmospheric radicals (Jacobsan, 1999; Li et al., 2011; Mok et al., 2016), which ultimately
52 influences the atmospheric photochemistry process, the formation of secondary organic aerosol
53 (SOA), and therefore the regional air quality (Mohr et al., 2013; Laskin et al., 2015; Moise et
54 al., 2015). In addition, some components in BrC, such as nitrated aromatic compounds (NACs)
55 (Teich et al., 2017; Wang et al., 2018) and polycyclic aromatic hydrocarbons (PAHs)

56 (Samburova et al., 2016; Huang et al., 2018), have adverse effects on human health (Bandowe
57 et al., 2014; Shen et al., 2018). The significant effects of BrC on environment, climate, air
58 quality and living things call for more studies to understand its chemical characteristics, sources
59 and the links with optical properties.

60 Investigating the chemical composition of BrC at molecular level is necessary, because
61 even small amounts of compounds can have a significant effect on the light absorption
62 properties of BrC and profound atmospheric implication (Mohr et al., 2013; Zhang et al., 2013;
63 Teich et al., 2017; Huang et al., 2018). A number of studies have investigated the BrC
64 composition at molecular level (Mohr et al., 2013; Zhang et al., 2013; Chow et al., 2015;
65 Samburova et al., 2016; Lin et al., 2016, 2017, 2018; Teich et al., 2017; Huang et al., 2018; Lu
66 et al., 2019). For example, Zhang et al. (2013) measured 8 NACs in Los Angeles and found that
67 they contributed about 4% of water-soluble BrC absorption at 365 nm. Huang et al. (2018)
68 measured 18 PAHs and their derivatives in Xi'an and found that they accounted for on average
69 ~1.7% of the overall absorption of methanol-soluble BrC. A state-of-the-art high performance
70 liquid chromatography-photodiode array-high resolution mass spectrometry (HPLC-PDA-
71 HRMS) was applied to investigate the elemental composition of BrC chromophores in biomass
72 burning aerosol (Lin et al., 2016, 2017, 2018). [Lin et al. \(2016\) reported that in biofuels burning](#)
73 [samples \(sawgrass, peat, ponderosa pine, and black spruce\), about 40-60% of the bulk BrC](#)
74 [absorption in the wavelength range of 300-500 nm may be attributed to 20 strong chromophores](#)
75 [and in another study \(Lin et al., 2017\) they reported that nitroaromatic compounds accounted](#)
76 [for ~50% of the total absorption of water-soluble BrC during the biomass burning event in a](#)
77 [nationwide bonfire festival in Israel.](#) Despite these efforts, the molecular composition of
78 atmospheric BrC still remains largely unknown due to its complexity in emission sources and
79 formation processes.

80 Field observations and laboratory studies show that BrC has various sources, including
81 primary emissions such as combustion and secondary formation from various atmospheric
82 processes (Laskin et al., 2015). Biomass burning, including forest fires and burning of crop
83 residues, is considered as the main source of BrC (Teich et al., 2017; Lin et al., 2017). Coal
84 burning and vehicle emissions are also important primary sources of BrC (Yan et al., 2017; Xie

85 et al., 2017; Sun et al., 2017; Li et al., 2019; Song et al., 2019). Secondary BrC is produced
86 through multiple-phase reactions occurring in or between gas phase, particle phase, and cloud
87 droplets. For example, nitrification of aromatic compounds (Harrison et al., 2005; Lu et al.,
88 2011), oligomers of acid-catalyzed condensation of hydroxyl aldehyde (De Haan et al., 2009;
89 Shapiro et al., 2009), and reaction of ammonia (NH₃) or amino acids with carbonyls (De Haan
90 et al., 2011; Nguyen et al., 2013; Flores et al., 2014) can all produce BrC. Condensed phase
91 reactions and aqueous-phase reactions have also been found to be important formation
92 pathways for secondary BrC in ambient air (Gilardoni et al., 2016). In addition, atmospheric
93 aging processes can lead to either enhancement or bleaching of the BrC absorption (Lambe et
94 al., 2013; Lee et al., 2014; Zhong and Jang, 2014), further challenging the characterization of
95 BrC.

96 As the starting point of the Silk Road, Xi'an is an important inland city in northwestern
97 China experiencing severe particulate air pollution, especially during heating period with
98 enhanced coal combustion and biomass burning activities (Wang et al., 2016; Ni et al., 2018).
99 In this study, we performed spectroscopic measurement and chemical analysis of PM_{2.5} filter
100 samples in Xi'an to investigate: 1) seasonal variations in the light absorption properties and
101 chromophore composition of BrC, and their relationships; 2) sources of BrC in different seasons
102 based on positive matrix factorization (PMF) model with light-absorbing organic markers as
103 input species.

104 **2 Experimental**

105 **2.1 Aerosol sampling**

106 A total of 112 daily ambient PM_{2.5} filter samples were collected on pre-baked (780 °C, 3
107 h) quartz-fiber filters (20.3 × 25.4 cm, Whatman, QM-A, Clifton, NJ, USA) in November-
108 December 2015, April-May, July, October-November 2016, representing winter, spring,
109 summer and fall, respectively. Filter samples were collected using a Hi-Vol PM_{2.5} air sampler
110 (Tisch, Cleveland, OH) at a flow rate of 1.05 m³ min⁻¹ on the roof (~10 m above ground level,
111 34.22°N, 109.01°E) of the Institute of Earth Environment, Chinese Academy of Sciences,
112 which was surrounded by residential areas without large industrial activities. After collection,

113 the filter samples were wrapped in baked aluminum foils and stored in a freezer (-20 °C) until
114 further analysis.

115 **2.2 Light absorption measurement**

116 One punch of loaded filter (0.526 cm²) was taken from each sample and sonicated for 30
117 minutes in 10 mL of ultrapure water (> 18.2 MΩ · cm) or methanol (HPLC grade, J. T. Baker,
118 Phillipsburg, NJ, USA). The extracts were then filtered with a 0.45 μm PTFE pore syringe filter
119 to remove insoluble materials. The light absorption spectra of water-soluble and methanol-
120 soluble BrC were measured with an UV-Vis spectrophotometer (300-700 nm) equipped with a
121 liquid waveguide capillary cell (LWCC-3100, World Precision Instrument, Sarasota, FL, USA)
122 following the method by Hecobian et al. (2010). The measured absorption data can be converted
123 to the absorption coefficient Abs_λ (M m⁻¹) by equation (1):

$$124 \quad \text{Abs}_\lambda = (A_\lambda - A_{700}) \frac{V_1}{V_a \times L} \times \ln(10) \quad (1)$$

125 where A₇₀₀ is the absorption at 700 nm, serving as a reference to account for baseline drift, V₁
126 is the volume of water or methanol that the filter was extracted into, V_a is the volume of sampled
127 air, L is the optical path length (0.94 m). A factor of ln(10) is used to convert the log base-10
128 (recorded by UV-Vis spectrophotometer) to natural logarithm to provide base-e absorption
129 coefficient. The absorption coefficient of water-soluble or methanol-soluble organics at 365 nm
130 (Abs₃₆₅) is used to represent water-soluble or methanol-soluble BrC absorption, respectively.

131 The mass absorption efficiency (MAE: m² gC⁻¹) of BrC in the extracts can be calculated
132 as:

$$133 \quad \text{MAE}_\lambda = \frac{\text{Abs}_\lambda}{M} \quad (2)$$

134 where M (μgC m⁻³) is the concentration of water-soluble organic carbon (WSOC) for water
135 extracts or methanol-soluble organic carbon (MSOC) for methanol extracts. Note that organic
136 carbon (OC) is often used to replace MSOC because direct measurement of MSOC is
137 technically difficult and many studies have shown that most of OC (~ 90%) can be extracted
138 by methanol (Chen and Bond, 2010; Cheng et al., 2016; Xie et al., 2019).

139 The wavelength-dependent light absorption of chromophores in solution, termed as
140 absorption Ångström exponent (AAE), can be described as:

141
$$\text{Abs}_\lambda = K \cdot \lambda^{-\text{AAE}} \quad (3)$$

142 where K is a constant related to the concentration of chromophores and AAE is calculated by
143 linear regression of $\log \text{Abs}_\lambda$ versus $\log \lambda$ in the wavelength range of 300-410 nm.

144 **2.3 Chemical analysis**

145 OC was measured with a thermal/optical carbon analyzer (DRI, model 2001) following
146 the IMPROVE-A protocol (Chow et al., 2011). WSOC was measured with a TOC/TN analyzer
147 (TOC-L, Shimadzu, Japan) (Ho et al., 2015).

148 Organic compounds listed in Table S1 were analyzed with a gas chromatograph-mass
149 spectrometer (GC-MS, Agilent Technologies, Santa Clara, CA, USA). Prior to the GC-MS
150 analysis, the silylation derivatization was conducted using a routine method (e.g., Wang et al.,
151 2016; Al-Naiema and stone, 2017). Briefly, a quarter of 47 mm filter sample was ultrasonically
152 extracted with 2 mL of methanol for 15 minutes and repeated three times. The extracts were
153 filtered with a 0.45 μm PTFE syringe filter and then evaporated with a rotary evaporator to \sim 1
154 mL and dried with a gentle stream of nitrogen. Then, 50 μL of N,O-
155 bis(trimethylsilyl)trifluoroacetamide (BSTFA-TMCS; Fluka Analytical 99%) and 10 μL of
156 pyridine were added. The mixture was heated for 3 h at 70 $^\circ\text{C}$ for silylation. After reaction, 140
157 μL of n-hexane were added to dilute the derivatives. Finally, 2 μL aliquot of the derivatized
158 extracts were introduced into the GC-MS, which was equipped with a DB-5MS column
159 (Agilent Technologies, Santa Clara, CA, USA), electron impact (EI) ionization source (70 eV),
160 and a GC inlet of 280 $^\circ\text{C}$. The GC oven temperature was held at 50 $^\circ\text{C}$ for 2 min, ramped to 120
161 $^\circ\text{C}$ at a rate of 15 $^\circ\text{C min}^{-1}$, and finally reached 300 $^\circ\text{C}$ at a rate of 5 $^\circ\text{C min}^{-1}$ (held for 16 min).
162 Note that the derivatization for NACs was conducted at 70 $^\circ\text{C}$ for 3 h which is slightly different
163 from the protocol used in Al-Naiema and stone (2017), because symmetrical peak shapes and
164 high intensities for NACs can also be obtained under this condition in our study (see Fig. S1).
165 In our study, 4-nitrophenol-2,3,5,6-d4 was used as an internal standard to correct for potential
166 loss for NACs quantification (Chow et al., 2015). For the quantification of other organic
167 compounds, an external standard method was used through daily calibration with working
168 standard solutions. Also, for every 10 samples, a procedural blank and a spiked sample (i.e.,
169 ambient sample spiked with known amounts of standards) were measured to check the

170 interferences and recoveries. The measured recoveries ~~were~~ are 80-102% and the uncertainties
171 (RSDs) ~~were~~ are < 10% for measured organic compounds.

172 2.4 Source apportionment of BrC

173 Source apportionment of methanol-soluble BrC was performed using positive matrix
174 factorization (PMF) as implemented by the multilinear engine (ME-2; Paatero, 1997) via the
175 Source Finder (SoFi) interface written in Igor Wavemetrics (Canonaco et al., 2013). Abs_{365,MSOC}
176 and those light-absorbing species including fluoranthene (FLU), pyrene (PYR), chrysene
177 (CHR), benzo(a)anthracene (BaA), benzo(a)pyrene (BaP), benzo(b)fluoranthene (BbF),
178 benzo(k)fluoranthene (BkF), indeno[1,2,3-cd]pyrene (IcdP), benzo(ghi)perylene (BghiP), 9,10-
179 anthracenequinone (9,10AQ), benzanthrone (BEN), benzo[b]fluoren-11-one (BbF11O),
180 vanillic acid, vanillin and syringyl acetone were used as model inputs, together with some
181 commonly used markers, i.e., phthalic acid, hopanes (17 α (H),21 β (H)-30-norhopane,
182 17 α (H),21 β (H)-hopane, 17 α (H),21 β (H)-(22S)-homohopane, 17 α (H),21 β (H)-(22R)-
183 homohopane, referred to as HP1-HP4, respectively), picene, and levoglucosan. The input data
184 include species concentrations and uncertainties. The ~~LOD (limit of detection) method detection~~
185 ~~limits (MDLs)~~, calculated as three times of the standard deviation of the blank filters, were used
186 to estimate species-specific uncertainties, following Liu et al. (2017). Furthermore, for a clear
187 separation of sources profiles, the contribution of corresponding markers was set to 0 in the
188 sources unrelated to the markers (see Table S2). This source apportionment protocol is very
189 similar to our previous study (Huang et al., 2014).

190 3 Results and discussion

191 3.1 Light absorption properties of water- and methanol-soluble BrC

192 Fig. 1 shows the temporal profiles of Abs₃₆₅ of water- and methanol-soluble BrC, together
193 with the concentrations of WSOC and OC (representing MSOC). They all show similar
194 seasonal variations with the highest average in winter, followed by fall, spring and summer (see
195 Table S3). WSOC contributed annually $54.4 \pm 16.2\%$ of the OC mass, with the highest
196 contribution in summer ($66.1 \pm 15.5\%$) and the lowest contribution in winter ($45.1 \pm 10.2\%$).
197 The higher WSOC fraction in OC during summer is largely contributed by SOA and to some

198 extent by biomass burning emissions because both SOA and biomass burning OA consist of
199 high fraction of WSOC (Ram et al., 2012; Yan et al., 2015; Daellenbach et al., 2016). The lower
200 WSOC fractions in OC during winter could be attributed to enhanced emissions from coal
201 combustion which produce a large fraction of water-insoluble organics (Daellenbach et al.,
202 2016; Yan et al., 2017). $Abs_{365,MSOC}$ is approximately 2 times (range 1.7-2.3) higher than
203 $Abs_{365,WSOC}$, which is similar to the results measured in Beijing (Cheng et al., 2016),
204 southeastern Tibetan Plateau (Zhu et al., 2018), Gwangju, Korea (Park et al., 2018) and the
205 Research Triangle Park, USA (Xie et al., 2019), indicating that the optical properties of BrC
206 could be largely underestimated when using water as the extracting solvent as non-polar
207 fraction of BrC is also important to light absorption of BrC (Sengupta et al., 2018). In Fig. S2
208 we summarized those previously reported $Abs_{365,WSOC}$ (as $Abs_{365,MSOC}$ was not commonly
209 measured in many previous studies) values at different sites in Asian urban and remote areas
210 and the US. $Abs_{365,WSOC}$ is significantly higher in most Asian urban regions than in the Asian
211 remote sites and the US, and show clear seasonal variations. The high light absorption of BrC
212 in Asian urban regions, especially during winter, may have important effects on regional climate
213 and radiation forcing (Park et al., 2010; Laskin et al., 2015). As discussed in Feng et al. (2013),
214 the average global climate forcing of BrC was estimated to be 0.04-0.11 $W m^{-2}$ and above 0.25
215 $W m^{-2}$ in urban sites of south and east Asia regions, which is about 25% of the radiative forcing
216 of black carbon (BC, 1.07 $W m^{-2}$). Thus, to further understand the influence of BrC on regional
217 radiation forcing, it is essential to identify and quantify the sources of BrC in Asia.

218 The seasonal averages of AAE of water-soluble BrC were between 5.32 and 6.15 without
219 clear seasonal trend (see Table S3). The seasonal averages of AAE of methanol-soluble BrC
220 were relatively lower than those of water-soluble BrC, ranging from 4.45 to 5.18 which is
221 similar to the results in Los Angeles Basin (Zhang et al., 2013) and Gwangju, Korea (Park et
222 al., 2018). This is because methanol can extract more [conjugated compounds that absorb](#)
223 [strongly at longer wavelengths \(e.g., PAHs\) with high conjugation degree and strong light-](#)
224 [absorbing capability \(e.g., PAHs\) at longer wavelength \(> 350 nm\)](#) (Samburova et al., 2016).
225 The AAE values of water-soluble BrC (as AAE of methanol-soluble BrC was not commonly
226 measured in many previous studies) in urban, rural and remote regions show a large difference

227 (see Fig. 2a), typically with much lower AAE values in urban regions than those in rural and
228 remote regions, indicating the difference in sources and chemical composition of chromophores.
229 The urban regions are mainly affected by anthropogenic emissions. Therefore, urban BrC may
230 contain a large amount of aromatic chromophores with high conjugation degree, which absorb
231 light at a longer wavelength and have lower AAE values (Lambe et al., 2013; Wang et al., 2018).

232 The average MAE_{365} values of water- and methanol-soluble BrC show large seasonal
233 variations, with highest values in winter (1.85 and 1.50 $m^2 gC^{-1}$, respectively), followed by fall
234 (1.18 and 1.52 $m^2 gC^{-1}$), spring (1.01 and 0.79 $m^2 gC^{-1}$), and summer (0.91 and 1.21 $m^2 gC^{-1}$).
235 Such large seasonal differences indicate seasonal difference in BrC sources. For example,
236 contributions from coal burning and biomass burning were much larger in winter than in other
237 seasons due to large residential heating activities (also see Section 3.3 for more details).
238 Compared to previous studies (Fig. 2b), the average values of $MAE_{365,WSOC}$ are obviously higher
239 in urban sites than in rural and remote sites that are less influenced by anthropogenic activities.
240 The higher $MAE_{365,WSOC}$ values in urban regions is likely associated with enhanced
241 anthropogenic emissions from e.g., coal combustion and biomass burning, and the lower
242 $MAE_{365,WSOC}$ values in rural and remote regions could be attributed to biogenic sources or aged
243 secondary BrC (Lei et al., 2018; Xie et al., 2019).

244 **3.2 Chemical characterization of the BrC chromophores**

245 Given the complexity in emission sources and formation processes, the molecular
246 composition of atmospheric BrC remains largely unknown. PAHs, NACs and MOPs have
247 recently been found as major chromophores in biomass burning-derived BrC (Lin et al., 2016,
248 2017, 2018). However, these compounds can also be directly emitted by coal combustion and
249 motor vehicle or formed by secondary reactions (Harrison et al., 2005; Iinuma et al., 2010; Liu
250 et al., 2017; Wang et al., 2018; Lu et al., 2019), making source attribution of atmospheric BrC
251 more challenging. To obtain the exact molecular composition of BrC chromophores and
252 understand the influence of a specific chromophore on BrC optical property, we measured the
253 light absorption characteristics of available chromophore standards including 12 PAHs, 10
254 NACs and 3 MOPs, and quantified their concentrations in $PM_{2.5}$ samples with GC-MS. The
255 light absorption contribution of individual chromophores to that of methanol-soluble BrC in the

256 wavelength range of 300-500 nm was estimated according to its concentration and mass
257 absorption efficiency (see Supplementary). Fig. 3 shows the contribution of carbon content in
258 identified BrC chromophores to the total OC mass. They all show obvious seasonal variations
259 with the highest values in winter and lowest in summer. The seasonal difference can be up to a
260 factor of 5-6. The contribution of PAHs ranged from 0.12% in summer to 0.47% in winter,
261 NACs from 0.02% in summer to 0.13% in winter, and MOPs from 0.01% in summer to 0.06%
262 in winter. It should be noted that NACs are dominated by 4-nitrophenol and 4-nitrocatechol in
263 spring, fall and winter, but by 4-nitrophenol and 5-nitrosalicylic acid in summer. The difference
264 is likely due to enhanced summertime formation of 5-nitrosalicylic acid, which is more oxidized
265 than other nitrated phenols measured in this study (Wang et al., 2018).

266 The seasonally averaged contributions of PAHs, NACs, MOPs and total measured
267 chromophores to light absorption of methanol-soluble BrC between 300 to 500 nm are shown
268 in Fig. 4. They show large seasonal variations and wavelength dependence. Specifically, PAHs
269 made the largest contribution to BrC light absorption in fall, followed by winter, spring and
270 summer, and show two large absorption peaks at about 365 nm and 380 nm, which are mainly
271 associated with the absorption of BaP, BghiP, IcdP, FLU, BkF and BaA (see Fig. S3). Compared
272 to PAHs, NACs show the largest contribution in winter, followed by fall, spring and summer,
273 and exhibit only one absorption peak at about 320 nm in spring and summer and at about 330
274 nm in fall and winter. The red shift in the absorption peak could be attributed to the increase of
275 contributions from 4-nitrocatechol, 4-methyl-5-nitrocatechol and 3-methyl-5-nitrocatechol
276 which have absorption peak at about 330-350 nm (see Fig. S3). Different from PAHs and NACs,
277 MOPs contribute the most in winter, followed by spring, fall and summer, and only show one
278 absorption peak at about 310 nm. The difference in light absorption contributions of different
279 chromophores in different seasons reflects the difference in sources, emission strength and
280 atmospheric formation processes.

281 The total contributions of PAHs, NACs and MOPs to the light absorption of methanol-
282 soluble BrC ranged from 0.47% (summer) to 1.56% (winter) at the wavelength of 300-500 nm
283 and ranged from 1.05% (summer) to 3.26% (winter) at the wavelength of 365 nm (see Table 1).
284 The average contribution of PAHs to the BrC light absorption at 365 nm was 0.97% in summer

285 (the lowest) and 2.69% in fall (the highest), the contribution of NACs was 0.09% in summer
286 and 0.82% in winter, and the contribution of MOPs was 0.006% in summer and 0.024% in
287 winter. The low contributions of these measured chromophores to the light absorption of
288 methanol-soluble BrC are consistent with previous studies. For example, Huang et al. (2018)
289 measured 18 PAHs and their derivatives, which on average contributed ~1.7% of the overall
290 absorption of methanol-soluble BrC in Xi'an. Mohr et al. (2013) estimated the contribution of
291 five NACs to particulate BrC light absorption at 370 nm to be ~4% in Detling, UK. Zhang et
292 al. (2013) measured eight NACs, which accounted for ~4% of water-soluble BrC absorption at
293 365 nm in Los Angeles. Teich et al. (2017) determined eight NACs during six campaigns at five
294 locations in summer and winter, and founded that the mean contribution of NACs to water-
295 soluble BrC absorption at 370 nm ranged from 0.10% to 1.25% under acidic conditions and
296 from 0.13% to 3.71% under alkaline conditions. Slightly different from these previous studies,
297 we investigated the contributions of three groups of chromophores with different light-
298 absorbing properties to the light absorption of BrC, and provided further understanding in the
299 relationships between optical properties and chemical composition of BrC in the atmosphere.
300 For example, vanillin, which has negligible contribution to BrC light absorption at 365 nm, can
301 produce secondary BrC through oxidation and thus enhance the light absorption by a factor of
302 5-7 (Li et al., 2014; Smith et al., 2016). The contribution of PAHs to the light absorption of
303 methanol-soluble BrC at 365 nm was 5-13 times that of their mass fraction of carbon in OC, 6-
304 9 times for NACs, and 0.4-0.7 times for MOPs (4-8 times at 310 nm for MOPs). These results
305 further demonstrate that even a small amount of chromophores can have a disproportionately
306 high impact on the light absorption properties of BrC, and that the light absorption of BrC is
307 likely determined by a number of chromophores with strong light absorption ability (Kampf et
308 al., 2012; Teich et al., 2017). Of note, a large fraction of BrC chromophores are still not
309 identified so far, and more studies are therefore necessary to better understand the BrC
310 chemistry. Based on laboratory and ambient studies, imidazoles (Kampf et al., 2012; Teich et
311 al., 2016), quinones (Lee et al., 2014; Pillar et al., 2017), nitrogenous PAHs (Lin et al., 2016;
312 Lin et al., 2018), polyphenols (Lin et al., 2016; Pillar et al., 2017) and oligomers with higher
313 conjugation (Lin et al., 2014; Lavi et al., 2017) could be included in future studies.

314 3.3 Sources of BrC

315 Two approaches have been used to quantify the sources of BrC, including multiple linear
316 regression and receptor models such as PMF. For example, Washenfelder et al. (2015) utilized
317 multiple linear regression to determine the contribution of individual OA factors resolved by
318 PMF to OA light absorption in the southeastern America. Moschos et al. (2018) combined the
319 time series of PMF-resolved OA factors with the time series of light absorption of water-soluble
320 OA extract as model inputs to quantify the sources of BrC in Magadino and Zurich, Switzerland.
321 Xie et al. (2019) quantified the sources of BrC in southeastern America using Abs₃₆₅, elemental
322 carbon (EC), OC, WSOC, isoprene sulfate ester, monoterpene sulfate ester, levoglucosan and
323 isoprene SOA tracers as PMF model inputs. However, it should be noted that previous studies
324 mainly rely on the correlation between measured light absorption and organic tracers that do
325 not contain a BrC chromophore, and therefore may lead to bias in BrC source apportionment.
326 To better constrain the sources of BrC (i.e., contribution to Abs_{365,MSOC}), we used BrC
327 chromophores as PMF model inputs. The inputs include vanillic acid, vanillin, and syringyl
328 acetone for BrC from biomass burning, and FLU, PYR, CHR, BaA, BaP, BbF, BkF, IcdP, BghiP,
329 for BrC from incomplete combustion and other light absorbing chromophores 9,10AQ, BEN,
330 and BbF11O. In addition, we included commonly used markers levoglucosan for biomass
331 burning, phthalic acid for secondary BrC, hopanes for vehicle emission and picene for coal
332 burning in the model inputs.

333 Four factors were resolved, including vehicle emission, coal burning, biomass burning and
334 secondary formation. The uncertainties for PMF analysis ~~were~~ [were](#) < 10% for secondary
335 formation and biomass burning, < 15% for vehicle emission and coal burning. The profile of
336 each factor is shown in Fig. S4. The first factor is characterized by a high contribution of
337 phthalic acid, a tracer of secondary formation of OA. The second factor is dominated by
338 hopanes, mainly from vehicular emissions. The third factor is characterized by high
339 contributions of PI, BaP, BbF, BkF, IcdP, BghiP, mainly from coal combustion emissions, while
340 the fourth factor has high contributions of levoglucosan, vanillic acid, vanillin, syringyl acetone
341 from biomass burning emissions. The seasonal difference in relative contribution of each factor
342 to BrC light absorption is shown in Fig. 5. In spring, vehicular emissions (34%) and secondary

343 formation (37%) were the main contributors to BrC and coal combustion also had a relatively
344 large contribution (29%). In summer, secondary formation constituted the largest fraction
345 (~60%), mainly due to enhanced photochemical formation of secondary BrC. In fall, vehicular
346 emissions (38%), coal combustion (29%) and biomass burning (22%) all had significant
347 contributions to BrC. In winter, coal combustion (44%) and biomass burning (36%) were the
348 main contributors, due to emissions from residential biomass burning (wood and crop residues)
349 and coal combustion for heating. In terms of absolute contributions to absorption of MSOC at
350 365 nm (see Table S4), secondary formation contributed 1.75, 2.55, 1.70, 6.20 M m⁻¹ in spring,
351 summer, fall and winter, respectively. The high contribution in winter can be attributed to
352 abundant precursors (volatile organic compounds) co-emitted with other primary sources
353 (especially coal burning and biomass burning), while the high contribution in summer might be
354 due to strong photochemical activity. For spring and fall, the absolute contributions from
355 secondary formation were very similar, indicating moderate precursor emission and moderate
356 photochemical activity. Also it should be noted that the absolute contributions of vehicle
357 emission to absorption of MSOC at 365 nm were still higher in spring and fall than those in
358 summer and winter, yet these differences by a factor of 2-9 are still less pronounced than the
359 differences (spring/fall vs. winter) for other primary emissions (> 40 times for coal burning
360 and > 25 times for biomass burning). In particular, the high vehicle contribution in fall might
361 be affected by high relative humidity in fall (83% in fall vs. 61-69% in other seasons, on average)
362 resulting in high vehicular PM_{2.5} emissions (Chio et al., 2010). Such large seasonal difference
363 in emission sources and atmospheric processes of BrC indicates that more studies are required
364 to better understand the relationship between chemical composition, formation processes, and
365 light absorption properties of BrC.

366 **4 Conclusion**

367 The light absorption properties of water- and methanol-soluble BrC in different seasons
368 were investigated in Xi'an. The light absorption coefficient of methanol-soluble BrC was
369 approximately 2 times higher than that of water-soluble BrC at 365 nm, and had an average
370 MAE₃₆₅ value of 1.27 ± 0.46 m² gC⁻¹. The average MAE₃₆₅ value of water-soluble BrC was 1.19
371 ± 0.51 m² gC⁻¹, which is comparable to those in previous studies at urban sites but higher than

372 those in rural and remote areas. The seasonally averaged AAE values of water-soluble BrC
373 ranged from 5.32 to 6.15, which are higher than those of methanol-soluble BrC (between 4.45
374 and 5.18). In combination with previous studies, we found that AAE values of water-soluble
375 BrC were much lower in urban regions than those in rural and remote regions. The difference
376 of optical properties of BrC in different regions could be attributed to the difference in sources
377 and chemical composition of BrC chromophores. The contributions of 12 PAHs, 10 NACs and
378 3 MOPs to the light absorption of methanol-soluble BrC were determined and showed large
379 seasonal variations. Specifically, the total contribution to methanol-soluble BrC light absorption
380 at 365 nm ranged from 1.1% to 3.3%, which is 5-7 times higher than their carbon mass fractions
381 in total OC. This result indicates that the light absorption of BrC is likely determined by an
382 amount of chromophores with strong light absorption ability. Four major sources of methanol-
383 soluble BrC were identified, including secondary formation, vehicle emission, coal combustion
384 and biomass burning. On average, secondary formation and vehicular emission were the main
385 contributors of BrC in spring (~70%). Vehicular emission (38%), coal burning (29%) and
386 biomass burning (22%) all contributed significantly to BrC in fall. Coal combustion and
387 biomass burning were the major contributors in winter (~80%), and secondary formation was
388 the predominant source in summer (~60%). The large variations of BrC sources in different
389 seasons suggest that more studies are needed to understand the seasonal difference in chemical
390 composition, formation processes, and light absorption properties of BrC, as well as their
391 relationships.

392 **5 Abbreviations of organics**

393 **PAHs (Polycyclic Aromatic Hydrocarbons)**

394	BaA	Benzo(a)anthracene
395	BaP	Benzo(a)pyrene
396	BbF	Benzo(b)fluoranthene
397	BbF11O	Benzo[b]fluoren-11-One
398	BEN	Benanthrone
399	BghiP	Benzo(ghi)perylene

400	BkF	Benzo(k)fluoranthene
401	CHR	Chrysene
402	FLU	Fluoranthene
403	IcdP	Indeno[1,2,3-cd]pyrene
404	PYR	Pyrene
405	9,10AQ	9,10-Anthracenequinone
406	NACs (Nitrated Aromatic Compounds)	
407	2M4NP	2-Methyl-4-Nitrophenol
408	2,6DM4NP	2,6-Dimethyl-4-Nitrophenol
409	3M4NP	3-Methyl-4-Nitrophenol
410	3M5NC	3-Methyl-5-Nitrocatechol
411	3NSA	3-Nitrosalicylic Acid
412	4M5NC	4-Methyl-5-Nitrocatechol
413	4NC	4-Nitrocatechol
414	4NP	4-Nitrophenol
415	4N1N	4-Nitro-1-Naphthol
416	5NSA	5-Nitrosalicylic Acid
417	MOP (Methoxyphenols)	
418	SyA	Syringyl Acetone
419	VaA	Vanillic Acid
420	VAN	Vanillin
421	Hopanes	
422	HP1	17 α (H),21 β (H)-30-Norhopane
423	HP2	17 α (H),21 β (H)-Hopane
424	HP3	17 α (H),21 β (H)-(22S)-Homohopane
425	HP4	17 α (H),21 β (H)-(22R)-Homohopane

426 *Data availability.* Raw data used in this study are archived at the Institute of Earth Environment,
427 Chinese Academy of Sciences, and are available on request by contacting the corresponding
428 author.

429 *Supplement.* The Supplement related to this article is available online at

430 *Author contributions.* RJH designed the study. Data analysis was done by WY, LY, and RJH.
431 WY, LY and RJH interpreted data, prepared the display items and wrote the manuscript. All
432 authors commented on and discussed the manuscript.

433 *Acknowledgements.* This work was supported by the National Natural Science Foundation of
434 China (NSFC) under grant no. 41877408, 41925015, and no. 91644219, the Chinese Academy
435 of Sciences (no. ZDBS-LY-DQC001), the Cross Innovative Team fund from the State Key
436 Laboratory of Loess and Quaternary Geology (SKLLQG) (no. SKLLQGTD1801), and the
437 National Key Research and Development Program of China (no. 2017YFC0212701). Yongjie
438 Li acknowledges funding support from the National Natural Science Foundation of China
439 (41675120), the Science and Technology Development Fund, Macau SAR (File no.
440 016/2017/A1), and the Multi-Year Research grant (No. MYRG2018-00006-FST) from the
441 University of Macau.

442 **References**

443 Al-Naiema, I. M., and Stone, E. A.: Evaluation of anthropogenic secondary organic aerosol
444 tracers from aromatic hydrocarbons, *Atmos. Chem. Phys.*, 17, 2053-2065,
445 doi:10.5194/acp-17-2053-2017, 2017.

446 Bandowe, B. A. M., Meusel, H., Huang, R.-J., Ho, K., Cao, J., Hoffmann, T., and Wilcke, W.:
447 PM_{2.5}-bound oxygenated PAHs, nitro-PAHs and parent-PAHs from the atmosphere of a
448 Chinese megacity: Seasonal variation, sources and cancer risk assessment, *Sci. Total*
449 *Environ.*, 473-474, 77-87, 2014.

450 Bosch, C., Andersson, A., Kirillova, E. N., Budhavant, K., Tiwari, S., Praveen, P. S., Russell,
451 L. M., Beres, N. D., Ramanathan, V., and Gustafsson, Ö.: Source-diagnostic dual-isotope
452 composition and optical properties of water-soluble organic carbon and elemental carbon

453 in the South Asian outflow intercepted over the Indian Ocean, *J. Geophys. Res. Atmos.*,
454 119, 11743-11759, doi:10.1002/2014JD022127, 2014.

455 Chen, Y., and Bond, T. C.: Light absorption by organic carbon from wood combustion, *Atmos.*
456 *Chem. Phys.*, 10, 1773-1787, doi:10.5194/acp-10-1773-2010, 2010.

457 Chen, Y., Ge, X., Chen, H., Xie, X., Chen, Y., Wang, J., Ye, Z., Bao, M., Zhang, Y., and Chen,
458 M.: Seasonal light absorption properties of water-soluble brown carbon in atmospheric
459 fine particles in Nanjing, China, *Atmos. Environ.*, 187, 230-240,
460 doi:10.1016/j.atmosenv.2018.06.002, 2018.

461 Cheng, Y., He, K. B., Du, Z. Y., Engling, G., Liu, J. M., Ma, Y. L., Zheng, M., and Weber, R. J.:
462 The characteristics of brown carbon aerosol during winter in Beijing, *Atmos. Environ.*,
463 127, 355-364, doi:10.1016/j.atmosenv.2015.12.035, 2016.

464 Choi, D., Beardsley, M., Brzezinski, D., Koupal, J., and Warila, J.: MOVES sensitivity analysis:
465 the impacts of temperature and humidity on emissions, [online] Available from:
466 <https://www3.epa.gov/ttnchie1/conference/ei19/session6/choi.pdf>, 2010.

467 Chow, J. C., Watson, J. G., Robles, J., Wang, X. L., Antony Chen, L. W., Trimble, D. L., Kohl,
468 S. D., Tropp, R. J., and Fung, K. K.: Quality assurance and quality control for
469 thermal/optical analysis of aerosol samples for organic and elemental carbon, *Anal.*
470 *Bioanal. Chem.*, 401, 3141- 3152, doi:10.1007/s00216-011-5103-3, 2011.

471 Chow, K. S., Huang, X. H. H., and Yu, J. Z.: Quantification of nitroaromatic compounds in
472 atmospheric fine particulate matter in Hong Kong over 3 years: field measurement
473 evidence for secondary formation derived from biomass burning emissions, *Environ.*
474 *Chem.*, 13, 665-673, doi:10.1071/EN15174, 2015.

475 Canonaco, F., Crippa, M., Slowik, J. G., Baltensperger, U., and Prévôt, A. S. H.: SoFi, an IGOR
476 based interface for the efficient use of the generalized multilinear engine (ME-2) for the
477 source apportionment: ME-2 application to aerosol mass spectrometer data, *Atmos. Meas.*
478 *Tech.*, 6, 3649-3661, doi:10.5194/amt-6-3649-2013, 2013.

479 Daellenbach, K. R., Bozzetti, C., Krepelova, A. K., Canonaco, F., Wolf, R., Zotter, P., Fermo,
480 P., Crippa, M., Slowik, J. G., Sosedova, Y., Zhang, Y., Huang, R. J., Poulain, L., Szidat, S.,
481 Baltensperger, U., El Haddad, I., and Prevot, A. S. H.: Characterization and source

482 apportionment of organic aerosol using offline aerosol mass spectrometry, *Atmos. Meas.*
483 *Tech.*, 9, 23-39, doi:10.5194/amt-9-23-2016, 2016.

484 De Haan, D. O., Corrigan, A. L., Smith, K. W., Stroik, D. R., Turley, J. J., Lee, F. E., Tolbert,
485 M. A., Jimenez, J. L., Cordova, K. E., and Ferrell, G. R.: Secondary organic aerosol-
486 forming reactions of glyoxal with amino acids, *Environ. Sci. Technol.*, 43, 2818-2824,
487 doi:10.1021/es803534f, 2009.

488 De Haan, D. O., Hawkins, L. N., Kononenko, J. A., Turley, J. J., Corrigan, A. L., Tolbert, M.
489 A., and Jimenez, J. L.: Formation of nitrogen-containing oligomers by methylglyoxal and
490 amines in simulated evaporating cloud droplets, *Environ. Sci. Technol.*, 45, 984-991,
491 doi:10.1021/es102933x, 2011.

492 Feng, Y., Ramanathan, V., and Kotamarthi, V. R.: Brown carbon: A significant atmospheric
493 absorber of solar radiation?, *Atmos. Chem. Phys.*, 13, 8607-8621, doi:10.5194/acp-13-
494 8607-2013, 2013.

495 Flores, J. M., Washenfelder, R. A., Adler, G., Lee, H. J., Segev, L., Laskin, J., Laskin, A.,
496 Nizkorodov, S. A., Brown, S. S., and Rudich, Y.: Complex refractive indices in the near-
497 ultraviolet spectral region of biogenic secondary organic aerosol aged with ammonia, *Phys.*
498 *Chem. Chem. Phys.*, 16, 10629-10642, doi:10.1039/c4cp01009d, 2014.

499 Gilardoni, S., Massoli, P., Paglione, M., Giulianelli, L., Carbone, C., Rinaldi, M., Decesari, S.,
500 Sandrini, S., Costabile, F., Gobbi, G. P., Pietrogrande, M. C., Visentin, M., Scotto, F., Fuzzi,
501 S., and Facchini, M. C.: Direct observation of aqueous secondary organic aerosol from
502 biomass-burning emissions, *Proc. Natl. Acad. Sci.*, 113, 10013-10018,
503 doi:10.1073/pnas.1602212113, 2016.

504 Harrison, M. A. J., Barra, S., Borghesi, D., Vione, D., Arsene, C., and Olariu, R. I.: Nitrated
505 phenols in the atmosphere: a review, *Atmos. Environ.*, 39, 231-248,
506 doi:10.1016/j.atmosenv.2004.09.044, 2005.

507 Hecobian, A., Zhang, X., Zheng, M., Frank, N. H., Edgerton, E. S., and Weber, R. J.: Water-
508 soluble organic aerosol material and the light absorption characteristics of aqueous extracts
509 measured over the Southeastern United States, *Atmos. Chem. Phys.*, 10, 5965-5977,
510 doi:10.5194/acp-10-5965-2010, 2010.

511 Ho, K. F., Ho, S. S. H., Huang, R. J., Liu, S. X., Cao, J. J., Zhang, T., Chuang, H. C., Chan, C.
512 S., Hu, D., and Tian, L.: Characteristics of water-soluble organic nitrogen in fine
513 particulate matter in the continental area of China, *Atmos. Environ.*, 106, 252-261,
514 doi:10.1016/j.atmosenv.2015.02.010, 2015.

515 Huang, R. J., Zhang, Y. L., Bozzetti, C., Ho, K. F., Cao, J. J., Han, Y. M., Daellenbach, K. R.,
516 Slowik, J. G., Platt, S. M., Canonaco, F., Zotter, P., Wolf, R., Pieber, S. M., Bruns, E. A.,
517 Crippa, M., Ciarelli, G., Piazzalunga, A., Schwikowski, M., Abbaszade, G., Schnelle-Kreis,
518 J., Zimmermann, R., An, Z. S., Szidat, S., Baltensperger, U., El Haddad, I., and Prévôt, A.
519 S. H.: High secondary aerosol contribution to particulate pollution during haze events in
520 China, *Nature*, 514, 218-222, 2014.

521 Huang, R. J., Yang, L., Cao, J., Chen, Y., Chen, Q., Li, Y., Duan, J., Zhu, C., Dai, W., Wang, K.,
522 Lin, C., Ni, H., Corbin, J. C., Wu, Y., Zhang, R., Tie, X., Hoffmann, T., O'Dowd, C., and
523 Dusek, U.: Brown carbon aerosol in urban Xi'an, Northwest China: the composition and
524 light absorption properties, *Environ. Sci. Technol.*, 52, 6825-6833,
525 doi:10.1021/acs.est.8b02386, 2018.

526 Iinuma, Y., Böge, O., Gräfe, R., and Herrmann, H.: Methyl-nitrocatechols: atmospheric tracer
527 compounds for biomass burning secondary organic aerosols, *Environ. Sci. Technol.*, 44,
528 8453-8459, doi:10.1021/Es102938a, 2010.

529 Jacobson, M. Z.: Isolating nitrated and aromatic aerosols and nitrated aromatic gases as sources
530 of ultraviolet light absorption, *J. Geophys. Res.*, 104, 3527-3542,
531 doi:10.1029/1998jd100054, 1999.

532 Kampf, C. J., Jakob, R., and Hoffmann, T.: Identification and characterization of aging products
533 in the glyoxal/ammonium sulfate system - implications for light-absorbing material in
534 atmospheric aerosols, *Atmos. Chem. Phys.*, 12, 6323-6333, doi:10.5194/acp-12-6323-
535 2012, 2012.

536 Kirillova, E. N., Andersson, A., Han, J., Lee, M., and Gustafsson, Ö.: Sources and light
537 absorption of water-soluble organic carbon aerosols in the outflow from northern China,
538 *Atmos. Chem. Phys.*, 14, 1413-1422, 2014a.

539 Kirillova, E. N., Andersson, A., Tiwari, S., Srivastava, A. K., Bisht, S. D., and Gustafsson, Ö.:

540 Water-soluble organic carbon aerosols during a full New Delhi winter: Isotope-based
541 source apportionment and optical properties, *J. Geophys. Res. Atmos.*, 119, 3476–3485,
542 2014b.

543 Lambe, A. T., Cappa, C. D., Massoli, P., Onasch, T. B., Forestieri, S. D., Martin, A. T.,
544 Cummings, M. J., Croasdale, D. R., Brune, W. H., Worsnop, D. R., and Davidovits, P.:
545 Relationship between oxidation level and optical properties of secondary organic aerosol,
546 *Environ. Sci. Technol.*, 47, 6349-6357, doi:10.1021/es401043j, 2013.

547 Laskin, A., Laskin, J., and Nizkorodov, S. A.: Chemistry of atmospheric brown carbon, *Chem.*
548 *Rev.*, 115, 4335-4382, doi:10.1021/cr5006167, 2015.

549 Lavi, A., Lin, P., Bhaduri, B., Carmieli, R., Laskin, A., and Rudich, Y.: Characterization of
550 Light-Absorbing Oligomers from Reactions of Phenolic Compounds and Fe(III), *ACS*
551 *Earth and Space Chemistry*, 1, 637-646, 2017.

552 Lee, H. J., Aiona, P. K., Laskin, A., Laskin, J., and Nizkorodov, S. A.: Effect of solar radiation
553 on the optical properties and molecular composition of laboratory proxies of atmospheric
554 brown carbon, *Environ. Sci. Technol.*, 48, 10217-10226, 2014.

555 Lei, Y. L., Shen, Z. X., Wang, Q. Y., Zhang, T., Cao, J. J., Sun, J., Zhang, Q., Wang, L. Q., Xu,
556 H. M., Tian, J., and Wu, J. M.: Optical characteristics and source apportionment of brown
557 carbon in winter PM_{2.5} over Yulin in Northern China, *Atmos. Res.*, 213, 27-33,
558 doi:10.1016/j.atmosres.2018.05.018, 2018.

559 Li, G., Bei, N., Tie, X., and Molina, L. T.: Aerosol effects on the photochemistry in Mexico
560 City during MCMA-2006/MILAGRO campaign, *Atmos. Chem. Phys.*, 11, 5169-5182,
561 doi:10.5194/acp-11-5169-2011, 2011.

562 Li, M. J., Fan, X. J., Zhu, M. B., Zou, C. L., Song, J. Z., Wei, S. Y., Jia, W. L., and Peng, P. A.:
563 Abundance and Light Absorption Properties of Brown Carbon Emitted from Residential
564 Coal Combustion in China, *Environ. Sci. Technol.*, 53, 595-603, 2019.

565 Li, Y. J., Huang, D. D., Cheung, H. Y., Lee, A. K. Y., and Chan, C. K.: Aqueous-phase
566 photochemical oxidation and direct photolysis of vanillin - a model compound of methoxy
567 phenols from biomass burning, *Atmos. Chem. Phys.*, 14, 2871-2885, doi:10.5194/acp-14-
568 2871-2014, 2014.

569 Lin, Y., Budisulistiorini, S. H., Chu, K., Siejack, R. A., Zhang, H., Riva, M., Zhang, Z., Gold,
570 A., Kautzman, K. E., and Surratt, J. D.: Light-Absorbing Oligomer Formation in
571 Secondary Organic Aerosol from Reactive Uptake of Isoprene Epoxydiols, *Environ. Sci.*
572 *Technol.*, 48, 12012-12021, doi:10.1021/es503142b, 2014.

573 Lin, P., Aiona, P. K., Li, Y., Shiraiwa, M., Laskin, J., Nizkorodov, S. A., and Laskin, A.:
574 Molecular characterization of brown carbon in biomass burning aerosol particles, *Environ.*
575 *Sci. Technol.*, 50, 11815-11824, doi:10.1021/acs.est.6b03024, 2016.

576 Lin, P., Bluvshstein, N., Rudich, Y., Nizkorodov, S. A., Laskin, J., and Laskin, A.: Molecular
577 chemistry of atmospheric brown carbon inferred from a nationwide biomass burning event,
578 *Environ. Sci. Technol.*, 51, 11561-11570, doi:10.1021/acs.est.7b02276, 2017.

579 Lin, P., Fleming, L. T., Nizkorodov, S. A., Laskin, J., and Laskin, A.: Comprehensive Molecular
580 Characterization of Atmospheric Brown Carbon by High Resolution Mass Spectrometry
581 with Electrospray and Atmospheric Pressure Photoionization, *Anal. Chem.*, 90, 12493-
582 12502, doi:10.1021/acs.analchem.8b02177, 2018.

583 Liu, Y., Yan, C. Q., Ding, X., Wang, X. M., Fu, Q. Y., Zhao, Q. B., Zhang, Y. H., Duan, Y. S.,
584 Qiu, X. H., and Zheng, M.: Sources and spatial distribution of particulate polycyclic
585 aromatic hydrocarbons in Shanghai, China, *Sci. Total Environ.*, 584-585, 307-317,
586 doi:10.1016/j.scitotenv.2016.12.134, 2017.

587 Lu, C., Wang, X., Li, R., Gu, R., Zhang, Y., Li, W., Gao, R., Chen, B., Xue, L., and Wang, W.:
588 Emissions of fine particulate nitrated phenols from residential coal combustion in China,
589 *Atmos. Environ.*, 203, 10-17, doi:10.1016/j.atmosenv.2019.01.047, 2019.

590 Lu, J. W., Michel Flores, J., Lavi, A., Abo-Riziq, A., and Rudich, Y.: Changes in the optical
591 properties of benzo[a]pyrene-coated aerosols upon heterogeneous reactions with NO₂ and
592 NO₃, *Phys. Chem. Chem. Phys.*, 13, 6484-6492, doi:10.1039/C0CP02114H, 2011.

593 Mohr, C., Lopez-Hilfiker, F. D., Zotter, P., Prevot, A. S. H., Xu, L., Ng, N. L., Herndon, S. C.,
594 Williams, L. R., Franklin, J. P., Zahniser, M. S., Worsnop, D. R., Knighton, W. B., Aiken,
595 A. C., Gorkowski, K. J., Dubey, M. K., Allan, J. D., and Thornton, J. A.: Contribution of
596 nitrated phenols to wood burning brown carbon light absorption in Detling, United
597 Kingdom during winter time, *Environ. Sci. Technol.*, 47, 6316-6324,

598 doi:10.1021/es400683v, 2013.

599 Moise, T., Flores, J. M., and Rudich, Y.: Optical properties of secondary organic aerosols and
600 their changes by chemical processes, *Chem. Rev.*, 115, 4400-4439, doi:10.1021/cr5005259,
601 2015.

602 Mok, J., Krotkov, N. A., Arola, A., Torres, O., Jethva, H., Andrade, M., Labow, G., Eck, T. F.,
603 Li, Z., Dickerson, R. R., Stenchikov, G. L., Osipov, S., and Ren, X.: Impacts of brown
604 carbon from biomass burning on surface UV and ozone photochemistry in the Amazon
605 Basin, *Sci. Rep.*, 6, 36940, doi:10.1038/srep36940, 2016.

606 Moschos, V., Kumar, N. K., Daellenbach, K. R., Baltensperger, U., Prévôt, A. S. H., and El
607 Haddad, I.: Source Apportionment of Brown Carbon Absorption by Coupling Ultraviolet-
608 Visible Spectroscopy with Aerosol Mass Spectrometry, *Environ. Sci. Tech. Lett.*, 5, 302-
609 308, doi:10.1021/acs.estlett.8b00118, 2018.

610 Nguyen, T. B., Laskin, A., Laskin, J., and Nizkorodov, S. A.: Brown carbon formation from
611 ketoaldehydes of biogenic monoterpenes, *Faraday Discuss.*, 165, 473-494,
612 doi:10.1039/C3FD00036B, 2013.

613 Ni, H. Y., Huang, R. J., Cao, J. J., Liu, W. G., Zhang, T., Wang, M., Meijer, H. A. J., and Dusek,
614 U.: Source apportionment of carbonaceous aerosols in Xi'an, China: insights from a full
615 year of measurements of radiocarbon and the stable isotope ^{13}C , *Atmos. Chem. Phys.*, 18,
616 16363-16383, doi:10.5194/acp-18-16363-2018, 2018.

617 Paatero, P.: Least squares formulation of robust non-negative factor analysis, *Chemom. Intell.*
618 *Lab.*, 37, 23-35, doi:10.1016/S0169-7439(96)00044-5, 1997.

619 Park, R. J., Kim, M. J., Jeong, J. I., Yooun, D., and Kim, S.: A contribution of brown carbon
620 aerosol to the aerosol light absorption and its radiative forcing in East Asia, *Atmos.*
621 *Environ.*, 44, 1414-1421, doi:10.1016/j.atmosenv.2010.01.042, 2010.

622 Park, S., Yu, G. H., and Lee, S.: Optical absorption characteristics of brown carbon aerosols
623 during the KORUS-AQ campaign at an urban site, *Atmos. Res.*, 203, 16-27,
624 doi:10.1016/j.atmosres.2017.12.002, 2018.

625 Pillar, E. A., and Guzman, M. I.: Oxidation of substituted catechols at the air-water interface:
626 Production of carboxylic acids, quinones, and polyphenols, *Environ. Sci. Technol.*, 51,

627 4951- 4959, <https://doi.org/10.1021/acs.est.7b00232>, 2017.

628 Ram, K., Sarin, M. M., and Tripathi, S. N.: Temporal trends in atmospheric PM_{2.5}, PM₁₀,
629 elemental carbon, organic carbon, water-soluble organic carbon, and optical properties:
630 impact of biomass burning emissions in the Indo-Gangetic Plain, *Environ. Sci. Technol.*,
631 46, 686-695, doi:10.1021/es202857w, 2012.

632 Samburova, V., Connolly, J., Gyawali, M., Yatavelli, R. L. N., Watts, A. C., Chakrabarty, R. K.,
633 Zielinska, B., Moosmüller, H., and Khlystov, A.: Polycyclic aromatic hydrocarbons in
634 biomass-burning emissions and their contribution to light absorption and aerosol toxicity,
635 *Sci. Total Environ.*, 568, 391-401, doi:10.1016/j.scitotenv.2016.06.026, 2016.

636 Samburova, V., Connolly, J., Gyawali, M., Yatavelli, R. L. N., Watts, A. C., Chakrabarty, R. K.,
637 Zielinska, B., Moosmüller, H., and Khlystov, A.: Polycyclic aromatic hydrocarbons in
638 biomass-burning emissions and their contribution to light absorption and aerosol toxicity,
639 *Sci. Total Environ.*, 568, 391-401, doi:10.1016/j.scitotenv.2016.06.026, 2016.

640 Sengupta, D., Samburova, V., Bhattarai, C., Kirillova, E., Mazzoleni, L., Iaukea-Lum, M.,
641 Watts, A., Moosmüller, H., and Khlystov, A.: Light absorption by polar and non-polar
642 aerosol compounds from laboratory biomass combustion, *Atmos. Chem. Phys.*, 18, 10849-
643 10867, doi:10.5194/acp-18-10849-2018, 2018.

644 Shapiro, E. L., Szprengiel, J., Sareen, N., Jen, C. N., Giordano, M. R., and McNeill, V. F.: Light-
645 absorbing secondary organic material formed by glyoxal in aqueous aerosol mimics,
646 *Atmos. Chem. Phys.*, 9, 2289-2300, doi:10.5194/acp-9-2289-2009, 2009.

647 Shen, M. L., Xing, J., Ji, Q. P., Li, Z. H., Wang, Y. H., Zhao, H. W., Wang, Q. R., Wang, T., Yu,
648 L. W., Zhang, X. C., Sun, Y. X., Zhang, Z. H., Niu, Y., Wang, H. Q., Chen, W., Dai, Y. F.,
649 Su, W. G., and Duan, H. W.: Declining Pulmonary Function in Populations with Long-
650 term Exposure to Polycyclic Aromatic Hydrocarbons-Enriched PM_{2.5}, *Environ. Sci.*
651 *Technol.*, 52, 6610-6616, 2018.

652 Smith, J. D., Kinney, H., and Anastasio, C.: Phenolic carbonyls undergo rapid aqueous
653 photodegradation to form low-volatility, light-absorbing products, *Atmos. Environ.*, 126,
654 36-44, doi:10.1016/j.atmosenv.2015.11.035, 2016.

655 Song, J. Z., Li, M. J., Fan, X. J., Zou, C. L., Zhu, M. B., Jiang, B., Yu, Z. Q., Jia, W. L., Liao,

656 Y. H., and Peng, P. A.: Molecular Characterization of Water- and Methanol-Soluble
657 Organic Compounds Emitted from Residential Coal Combustion Using Ultrahigh-
658 Resolution Electrospray Ionization Fourier Transform Ion Cyclotron Resonance Mass
659 Spectrometry, *Environ. Sci. Technol.*, 53, 13607-13617, doi:10.1021/acs.est.9b04331,
660 2019.

661 Srinivas, B., and Sarin, M. M.: Light-absorbing organic aerosols (brown carbon) over the
662 tropical Indian Ocean: impact of biomass burning emissions, *Environ. Res. Lett.*, 8,
663 044042, doi:10.1088/1748-9326/8/4/044042, 2013.

664 Sun, J., Zhi, G., Hitzenberger, R., Chen, Y., Tian, C., Zhang, Y., Feng, Y., Cheng, M., Zhang, Y.,
665 Cai, J., Chen, F., Qiu, Y., Jiang, Z., Li, J., Zhang, G., and Mo, Y.: Emission factors and
666 light absorption properties of brown carbon from household coal combustion in China,
667 *Atmos. Chem. Phys.*, 17, 4769-4780, doi:10.5194/acp-17-4769-2017, 2017.

668 Teich, M., van Pinxteren, D., Kecorius, S., Wang, Z., and Herrmann, H.: First quantification of
669 imidazoles in ambient aerosol particles: potential photosensitizers, brown carbon
670 constituents, and hazardous components, *Environ. Sci. Technol.*, 50, 1166-1173, 2016.

671 Teich, M., van Pinxteren, D., Wang, M., Kecorius, S., Wang, Z., Müller, T., Mocnik, G., and
672 Herrmann, H.: Contributions of nitrated aromatic compounds to the light absorption of
673 water-soluble and particulate brown carbon in different atmospheric environments in
674 Germany and China, *Atmos. Chem. Phys.*, 17, 1653-1672, doi:10.5194/acp-17-1653-2017,
675 2017.

676 Wang, G. H., Kawamura, K., Lee, S., Ho, K. F., and Cao, J. J.: Molecular, seasonal, and spatial
677 distributions of organic aerosols from fourteen Chinese cities, *Environ. Sci. Technol.*, 40,
678 4619-4625, doi:10.1021/es060291x, 2006.

679 Wang, J. Z., Ho, S. S. H., Huang, R. J., Gao, M. L., Liu, S. X., Zhao, S. Y., Cao, J. J., Wang, G.
680 H., Shen, Z. X., and Han, Y. M.: Characterization of parent and oxygenated-polycyclic
681 aromatic hydrocarbons (PAHs) in Xi'an, China during heating period: An investigation of
682 spatial distribution and transformation, *Chemosphere*, 159, 367-377,
683 doi:10.1016/j.chemosphere.2016.06.033, 2016.

684 Wang, L. W., Wang, X. F., Gu, R. R., Wang, H., Yao, L., Wen, L., Zhu, F. P., Wang, W. H., Xue,

685 L. K., Yang, L. X., Lu, K. D., Chen, J. M., Wang, T., Zhang, Y. H., and Wang, W. X.:
686 Observations of fine particulate nitrated phenols in four sites in northern China:
687 concentrations, source apportionment, and secondary formation, *Atmos. Chem. Phys.*, 18,
688 4349-4359, doi:10.5194/acp-18-4349-2018, 2018.

689 Washenfelder, R. A., Attwood, A. R., Brock, C. A., Guo, H., Xu, L., Weber, R. J., Ng, N. L.,
690 Allen, H. M., Ayres, B. R., Baumann, K., Cohen, R. C., Draper, D. C., Duffey, K. C.,
691 Edgerton, E., Fry, J. L., Hu, W. W., Jimenez, J. L., Palm, B. B., Romer, P., Stone, E. A.,
692 Wooldridge, P. J., and Brown, S. S.: Biomass burning dominates brown carbon absorption
693 in the rural southeastern United States, *Geophys. Res. Lett.*, doi:10.1002/2014GL062444,
694 42, 653-664, 2015.

695 Xie, M. J., Chen, X., Hays, M. D., Lewandowski, M., Offenberg, J., Kleindienst, T. E., and
696 Holder, A. L.: Light absorption of secondary organic aerosol: composition and
697 contribution of nitroaromatic compounds, *Environ. Sci. Technol.*, 51, 11607-11616,
698 doi:10.1021/acs.est.7b03263, 2017.

699 Xie, M. J., Chen, X., Holder, A. L., Hays, M. D., Lewandowski, M., Offenberg, J. H.,
700 Kleindienst, T. E., Jaoui, M., and Hannigan, M. P.: Light absorption of organic carbon and
701 its sources at a southeastern U.S. location in summer, *Environ. Pollut.*, 244, 38-46,
702 doi:10.1016/j.envpol.2018.09.125, 2019.

703 Yan, C. Q., Zheng, M., Sullivan, A. P., Bosch, C., Desyaterik, Y., Andersson, A., Li, X. Y., Guo,
704 X. S., Zhou, T., Gustafsson, O., and Collett Jr, J. L.: Chemical characteristics and light-
705 absorbing property of water-soluble organic carbon in Beijing: Biomass burning
706 contributions, *Atmos. Environ.*, 121, 4-12, doi:10.1016/j.atmosenv.2015.05.005, 2015.

707 Yan, C. Q., Zheng, M., Bosch, C., Andersson, A., Desyaterik, Y., Sullivan, A. P., Collett, J. L.,
708 Zhao, B., Wang, S. X., He, K. B., and Gustafsson, Ö.: Important fossil source contribution
709 to brown carbon in Beijing during winter, *Sci. Rep.*, 7, 43182, doi:10.1038/srep43182,
710 2017.

711 Zhang, X., Lin, Y.-H., Surratt, J. D., and Weber, R.: Sources, composition and absorption
712 Ångström exponent of light-absorbing organic components in aerosol extracts from the
713 Los Angeles Basin, *Environ. Sci. Technol.*, 47, 3685-3693, doi:10.1021/es305047b, 2013.

714 Zhang, Y., Forrister, H., Liu, J., Dibb, J., Anderson, B., Schwarz, J. P., Perring, A. E., Jimenez,
715 J. L., Campuzano-Jost, P., Wang, Y., Nenes, A., and Weber, R. J.: Top-of-atmosphere
716 radiative forcing affected by brown carbon in the upper troposphere, *Nat. Geosci.*, 10, 486-
717 489, doi:10.1038/NGEO2960, 2017a.

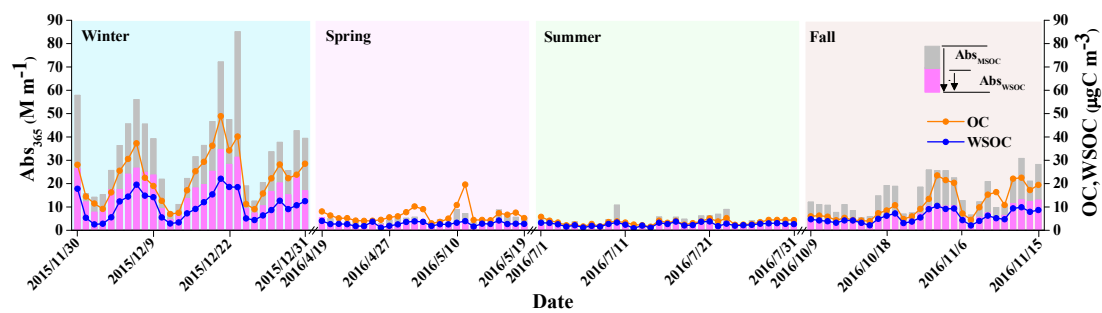
718 Zhang, Y., Xu, J., Shi, J., Xie, C., Ge, X., Wang, J., Kang, S., and Zhang, Q.: Light absorption
719 by water-soluble organic carbon in atmospheric fine particles in the central Tibetan Plateau,
720 *Environ. Sci. Pollut. Res.*, 24, 21386–21397, doi:10.1007/s11356-017-9688-8, 2017b.

721 Zhong, M., and Jang, M.: Dynamic light absorption of biomass-burning organic carbon
722 photochemically aged under natural sunlight, *Atmos. Chem. Phys.*, 14, 1517-1525, 2014.

723 Zhu, C. S., Cao, J. J., Huang, R. J., Shen, Z. X., Wang, Q. Y., and Zhang, N. N.: Light absorption
724 properties of brown carbon over the southeastern Tibetan Plateau, *Sci. Total Environ.*, 625,
725 246-251, doi:10.1016/j.scitotenv.2017.12.183, 2018.

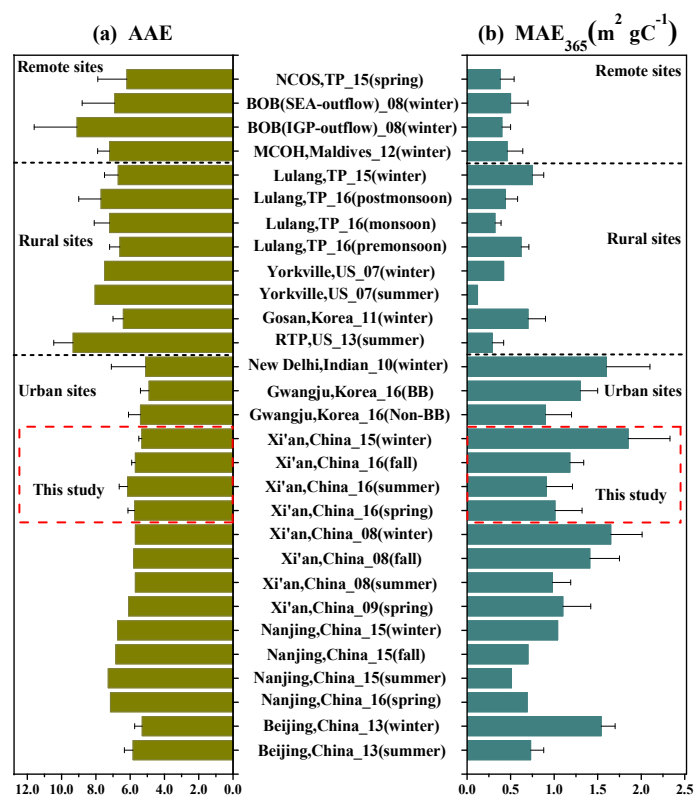
726 **Table 1.** Annual and seasonal mean contributions of measured PAHs, NACs and MOPs to
 727 methanol-soluble BrC light absorption at 365 nm. Hyphens denote the measured value of more
 728 than one third of the samples is below the detection limit.

Compounds	MAE ₃₆₅ (m ² gC ⁻¹)	Contribution to BrC light absorption at 365 nm (%)				
		Annual	Spring	Summer	Fall	Winter
Fluoranthene (FLU)	4.25	0.11	0.05	0.02	0.05	0.15
Pyrene (PYR)	0.46	0.01	0.00	0.00	0.01	0.01
Chrysene (CHR)	0.00	0.00	0.00	0.00	0.00	0.00
Benzo(a)anthracene (BaA)	2.06	0.04	0.01	0.01	0.02	0.05
Benzo(a)pyrene (BaP)	9.31	1.04	0.76	0.39	1.16	1.10
Benzo(b)fluoranthene (BbF)	4.10	0.17	0.14	0.07	0.17	0.18
Benzo(k)fluoranthene (BkF)	3.47	0.04	0.03	0.02	0.04	0.04
Indeno[1,2,3-cd]pyrene (IcdP)	4.68	0.51	0.50	0.24	0.71	0.46
Benzo(ghi)perylene (BghiP)	8.95	0.29	0.28	0.16	0.41	0.26
9,10-Anthracenequinone (9,10AQ)	0.28	0.01	0.00	0.00	0.00	0.01
Benzoanthrone (BEN)	6.13	0.11	0.08	0.05	0.11	0.12
Benzo[b]fluorene-11-one (BbF11O)	1.89	0.02	0.02	0.01	0.02	0.03
4-Nitrophenol (4NP)	2.17	0.08	0.06	0.02	0.05	0.10
4-Nitro-1-naphthol (4N1N)	9.71	-	-	-	-	0.03
2-Methyl-4-nitrophenol (2M4NP)	2.81	0.03	0.01	0.01	0.01	0.04
3-Methyl-4-nitrophenol (3M4NP)	2.65	0.02	0.01	0.00	0.01	0.03
2,6-Dimethyl-4-nitrophenol (2,6DM4NP)	3.27	-	-	-	-	0.01
4-Nitrocatechol (4NC)	7.91	0.27	0.05	0.03	0.20	0.35
3-Methyl-5-nitrocatechol (3M5NC)	5.77	-	-	-	0.05	0.11
4-Methyl-5-nitrocatechol (4M5NC)	7.29	-	-	-	0.06	0.13
3-Nitrosalicylic acid (3NSA)	3.86	-	-	-	-	0.01
5-Nitrosalicylic acid (5NSA)	3.36	0.03	0.01	0.02	0.04	0.02
Syringyl acetone (SyA)	0.25	0.01	0.01	0.00	0.01	0.01
Vanillin (VAN)	8.17	0.01	0.00	0.00	0.00	0.01
Vanillic acid (VaA)	0.66	0.00	0.00	0.00	0.00	0.00
Total	103.46	2.80	2.02	1.05	3.13	3.26

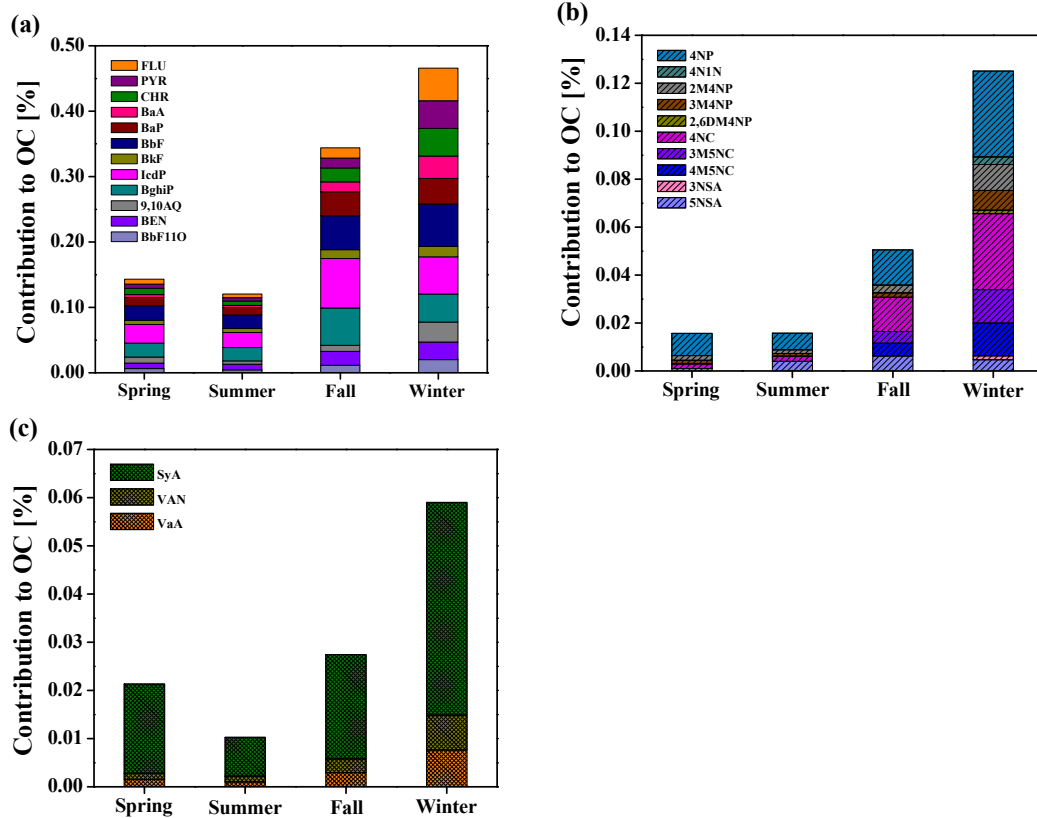


729

730 **Figure 1.** Time series of the light absorption coefficient of water-soluble and methanol-soluble
 731 BrC at 365 nm ($Abs_{365,WSOC}$ and $Abs_{365,MSOC}$, respectively), as well as OC and WSOC
 732 concentrations.



733 **Figure 2.** Comparison of AAE (left column) and MAE₃₆₅ (right column) values of water-soluble
 734 BrC at remote sites (Srinivas and Sarin, 2013; Bosch et al., 2014; Zhang et al., 2017b), rural
 735 sites (Hocobian et al., 2010; Kirillova et al., 2014a; Zhu et al., 2018; Xie et al., 2019) and urban
 736 sites (Kirillova et al., 2014b; Yan et al., 2015; Chen et al., 2018; Huang et al., 2018; Park et al.,
 737 2018).

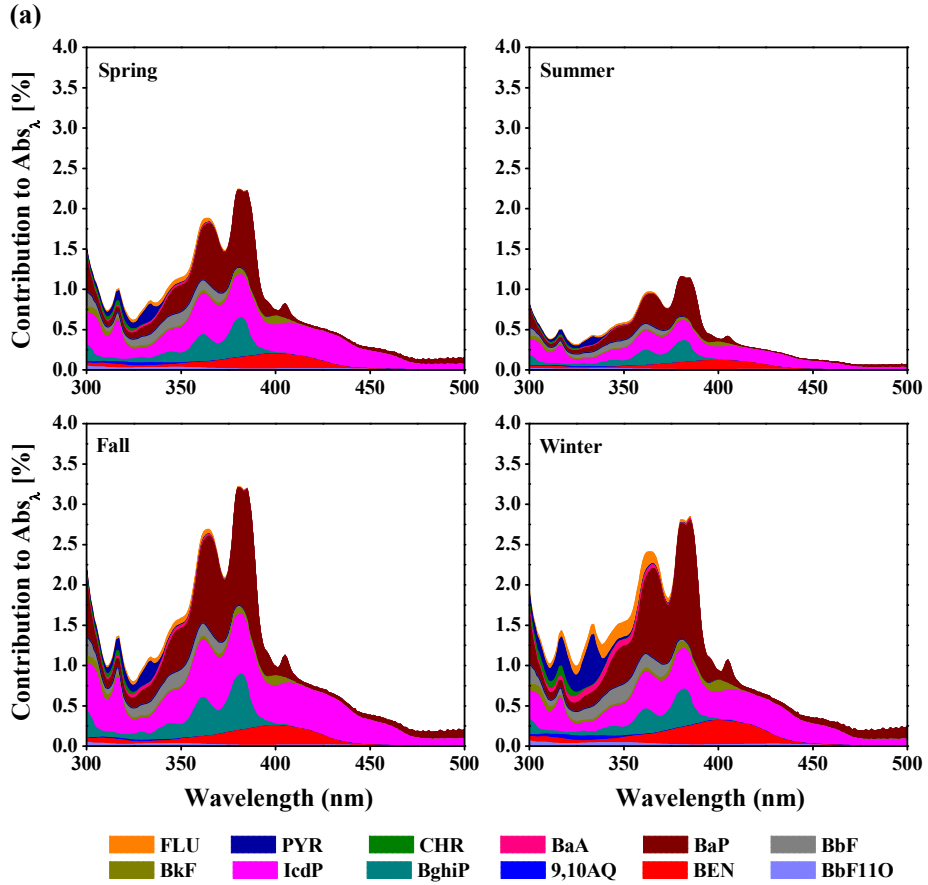


738

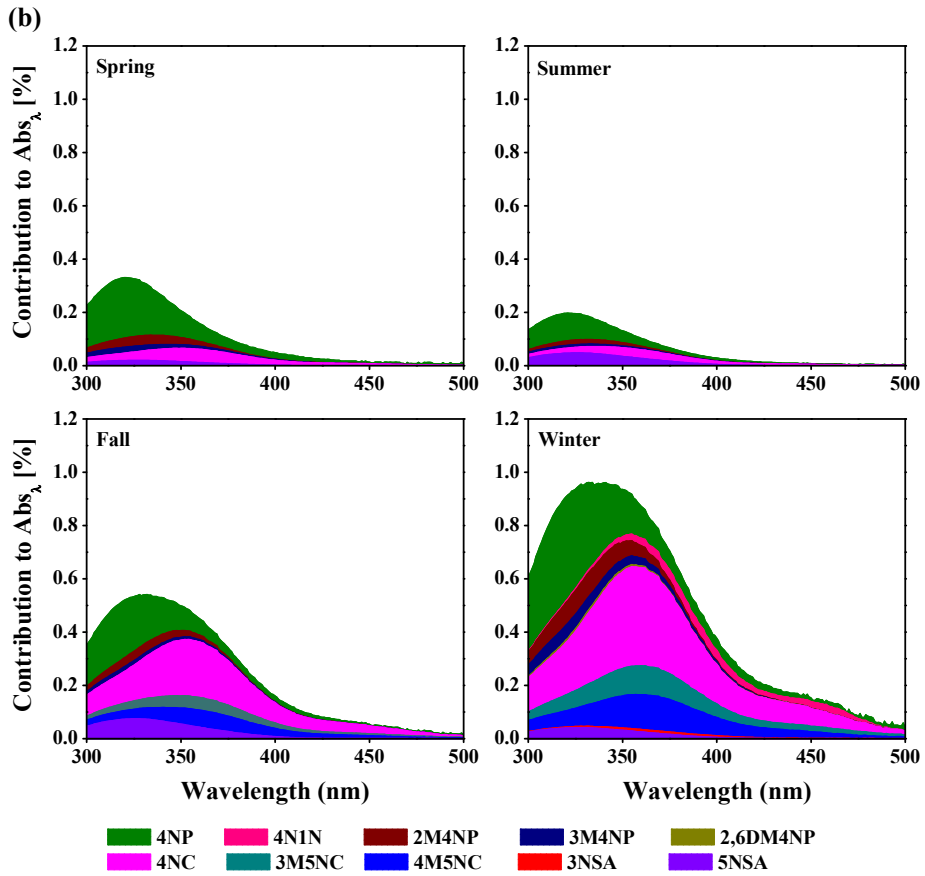
739
740

741 **Figure 3.** Contributions of (a) PAHs, (b) NACs, and (c) MOPs carbon mass concentrations to
742 the total OC concentrations.

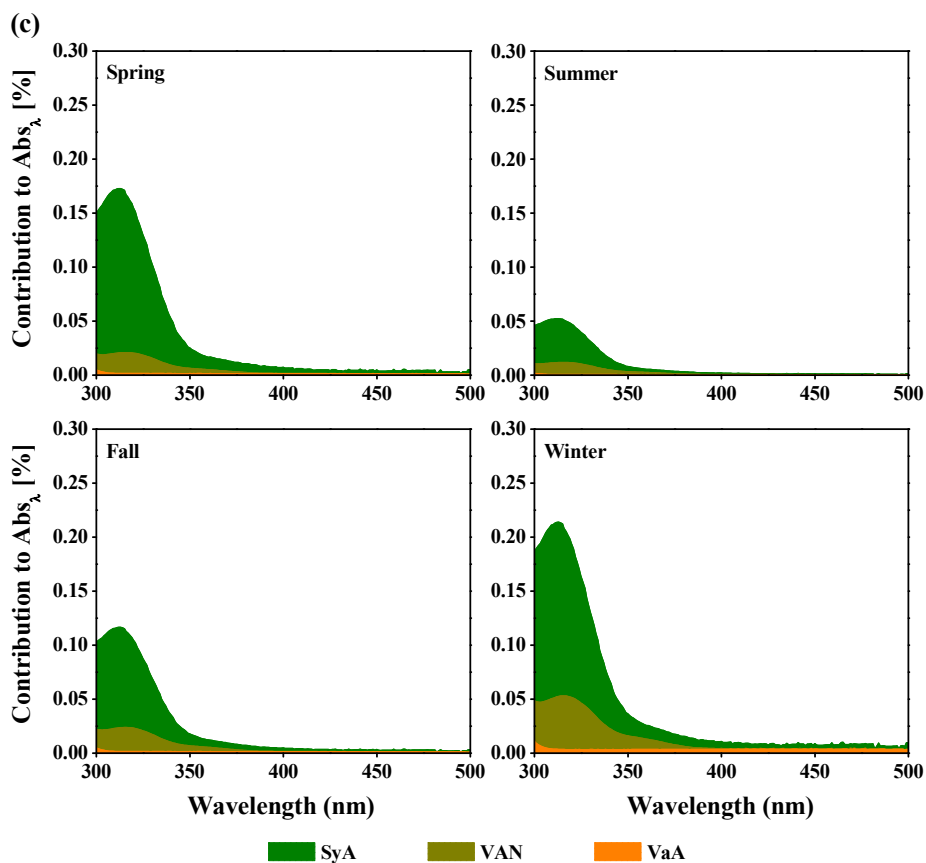
743



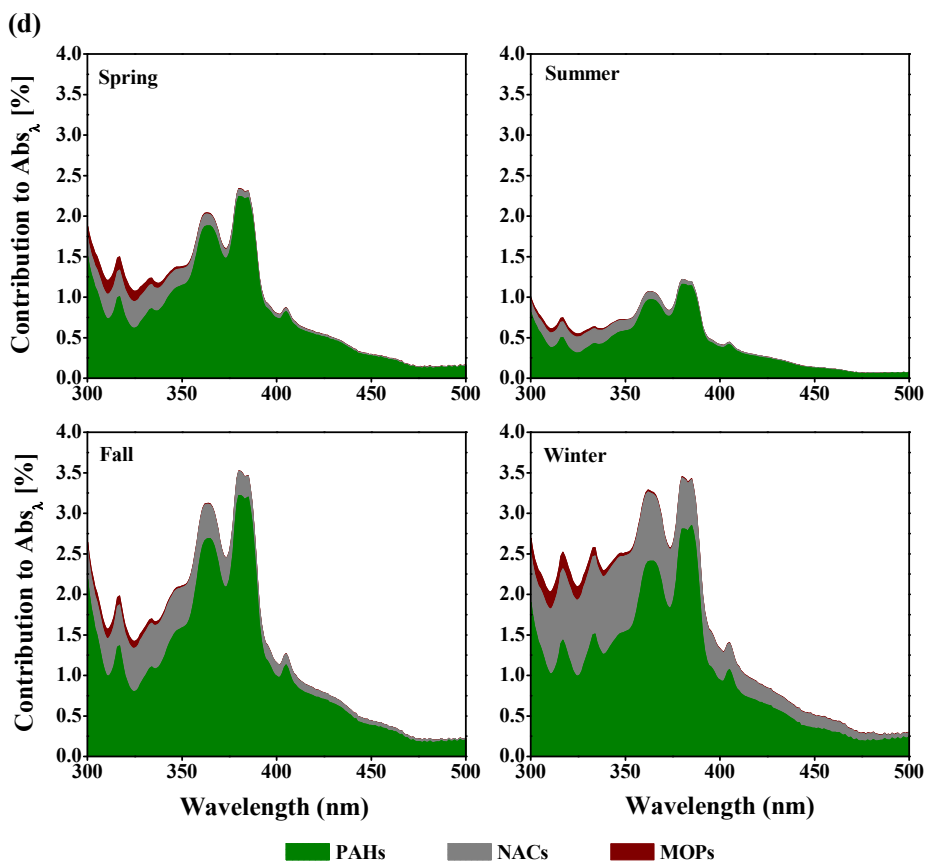
744



745



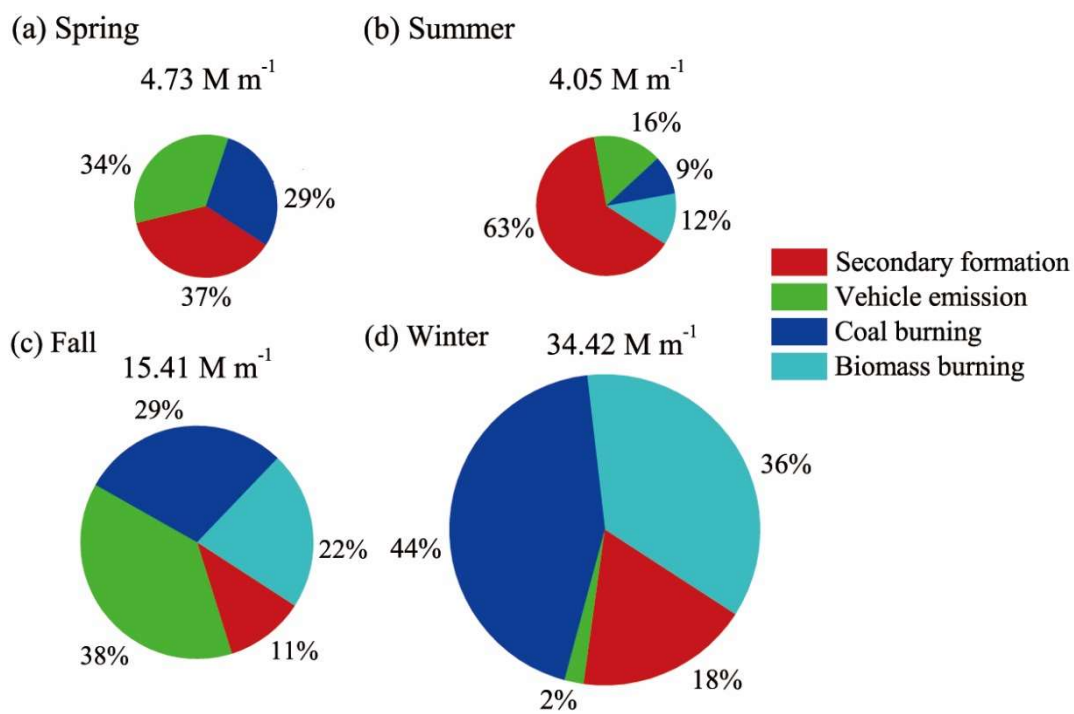
746



747

748 **Figure 4.** Light absorption contributions of (a) PAHs, (b) NACs, (c) MOPs and (d) total

749 measured chromophores to Abs_{MSOC} over the wavelength range of 300 to 500 nm in spring,
750 summer, fall and winter.
751



752

753 **Figure 5.** Contributions of the major sources to Abs_{365,MSOC} in Xi'an during spring, summer, fall

754 and winter.